

Second-order statically screened exchange correction to the random phase approximation: Assessment for non-covalent interactions

Arno Förster*

*Theoretical Chemistry, Vrije Universiteit, De Boelelaan 1083, NL-1081 HV, Amsterdam,
The Netherlands*

E-mail: a.t.l.foerster@vu.nl

Abstract

With increasing inter-electronic distance, the screening of the electron-electron interaction by the presence of other electrons becomes the dominant source of electron correlation. This effect is described by the random phase approximation (RPA) which is therefore a promising method for the calculation of weak interactions. The success of the RPA relies on the cancellation of errors, which can be traced back to the violation of the crossing symmetry of the 4-point vertex, leading to strongly overestimated total correlation energies. By addition of second-order screened exchange (SOSEX) to the correlation energy, this issue is substantially reduced. In the adiabatic connection (AC) SOSEX formalism, one of the two electron-electron interaction lines in the second-order exchange term is dynamically screened. A related SOSEX expression in which both electron-electron interaction lines are statically screened is obtained from the $G3W2$ contribution to the electronic self-energy. In contrast to AC-SOSEX, the evaluation of this correlation energy expression does not require an expensive numerical frequency integration and is therefore advantageous from a computational perspective. We compare the accuracy of both RPA+SOSEX variants for the calculation of the interaction

energies of non-covalently bound complexes. Both variants, independently of the input Kohn-Sham Green’s function, result in significant improvements over RPA. They are also comparable in accuracy, indicating that the dynamical screened effects are of minor importance in the description of long-ranged interactions. For dispersion interactions, both RPA+SOSEX variants are however outperformed by dispersion corrected hybrid and double-hybrid functionals.

1 Introduction

The random phase approximation (RPA)^{1,2} has found widespread use in quantum chemistry for the calculation of covalent and non-covalent interaction energies.^{3–11} The direct (particle-hole) RPA can be derived in the framework of the adiabatic connection (AC) fluctuation-dissipation theorem (ACFD)^{12–14} or as a subset of terms in the coupled cluster (CC)^{15–19} singles and doubles (CCD) expansion.^{20,21} Within Many-body perturbation theory (MBPT),^{22–25} the RPA is obtained by evaluating the Klein,²⁶ or alternatively, the Luttinger-Ward²⁷ functional with the self-energy in the *GW* approximation (GWA) using a (non-interacting) Kohn-Sham (KS)²⁸ Density functional theory (DFT)²⁹ Green’s function.^{30,31}

In the GWA,³² the self-energy is obtained as the first term of an expansion in terms of a screened electron-electron interaction where screening is usually calculated within a pair bubble approximation^{33,25} The RPA is generally believed to describe long-range electron correlation very accurately since the effect of charge screening dominates in this limit.¹³ This property is very desirable for the description of long-range dispersion effects or hydrogen bonding, which are omnipresent in chemistry and biology, determining for instance the structure of DNA or protein folding.^{34,35}

The magnitude of dispersion interactions does generally grow super-linearly with system size³⁶ and it’s relative importance compared to covalent bonding therefore increases with the number of electrons. Especially for larger systems, it becomes decisive to take into account the screening of the electron-electron interaction. CC and MBPT based methods

describe this screening by resummation of certain classes of self-energy diagrams to infinite order.^{23,37,38} The RPA is the simplest first principle method which accounts for these effects and is implemented with $\mathcal{O}(N^4)$ scaling with system size using global density fitting (DF).³⁹ Modern RPA (and *GW*) implementations typically use local density-fitting approaches to calculate the non-interacting polarizability,⁴⁰⁻⁴⁵ leading to quadratic or cubic scaling in practice, and even effectively linearly scaling implementations (for sufficiently sparse and large systems) have been reported.⁴⁶⁻⁴⁹ For these reasons, the RPA is considered a promising method to study non-covalent interactions⁵⁰⁻⁵⁴ also in large molecules.⁵⁵ At short electron-electron distances, however, charge screening becomes less important for the description of electron correlation and taking into account higher-order contributions to the self-energy via the 4-point vertex function becomes decisive.⁵⁶ The absence of these terms in the RPA leads to Pauli exclusion principle violating contributions to the electron correlation energy.⁵⁷ As a consequence, total correlation energies are much too high compared to exact reference values.^{58,59}

In contrast to RPA, the approximations to the correlation energy of Møller-Plesset perturbation theory (MPPT) are free of Pauli principle violating terms. Especially MP2 is relatively inexpensive and can routinely applied to systems with more than 100 atoms even close to the complete basis set limit. However, screening effects are entirely absent in MPPT and electron correlation is described by HF quasiparticles (QP) interacting via the bare Coulomb interaction instead, neglecting the fact that the interactions between the HF QPs are generally much weaker than the ones between the undressed electrons. This issue is also present in orbital optimized MP2 in which the HF QPs are replaced by MP2 QPs.⁶⁰⁻⁶² Therefore, MP2 is a suitable method only for (typically small) systems in which screening effects are negligible. The divergence of MPPT for the uniform electron gas (see for instance chapter 10 in ref. 23 for a thorough discussion) is known at least since early work by Macke¹ and has been demonstrated later on for metals⁶³ and recently also for large, non-covalently bound organic complexes.⁵⁵ The divergence of the Møller-Plesset series for small-gap systems

is directly related to this issue since the magnitude of the screening is proportional to the width of the fundamental gap.^{64,65}

There have been various approaches to regularize MP2 by an approximate treatment of higher-order screening effects, either using empirical^{34,66–75} or diagrammatically motivated modifications^{38,76–78} or attacking the problem from a DFT perspective.^{79,80} Starting from the opposite direction, there have been many attempts to correct the RPA correlation energy expression by adding additional terms to improve the description of short-range correlation. This includes range-separation based approaches,^{81–90} or augmentations by singles contributions.^{8,91,92} Via MBPT, the RPA can generally be improved upon inclusion of the 4-point vertex in the electronic self-energy, either directly, or indirectly through the kernel of the Bethe-Salpeter equation (BSE) for the generalized susceptibility. Following the latter approach, approximations often start from the ACFD and go beyond the Coulomb kernel in the BSE by adding additional terms, for instance exact exchange (exx) (often denoted as exx-RPA)^{93–99} and higher order contributions,^{100–102} or the statically screened *GW* kernel,^{103–105} but also empirically tuned functions of the eigenvalues of the KS density-density response.^{106,107} Notice, that the BSE for the generalized susceptibility reduces to a Dyson equation for the density-density response function which makes local kernels very attractive from a computational perspective.

Instead of relying on the ACFD theorem, beyond-RPA energy expressions can also be introduced directly from approximations to the self-energy beyond the GWA. For instance, in RPAX^{108–111} a local 4-point vertex obtained from the functional derivative of the *local* exact exchange potential calculated within the optimized effective potential method^{112–114} is used in the self-energy. In Freeman’s second-order screened exchange (SOSEX) correction,¹¹⁵ the HF vertex (i.e. the functional derivative of the *non-local* HF self-energy with respect to the single-particle Green’s function) is included in the self-energy directly but not in the screened interaction.^{8,57,92,116–118} Another expression for SOSEX can be obtained by including the static *GW* kernel in the self-energy but not in the density-density response. This possibility

has not been explored until recently¹¹⁹ and is the main topic of this work.

In our recent work, we have assessed the accuracy of the statically screened $G3W2$ correction to the GW self-energy for charged excitations.¹¹⁹ This correction has first been applied by Grüneis *at al.*¹²⁰ to calculate the electronic structure of solids and is obtained by calculating the self-energy to second-order in the screened Coulomb interaction (equivalent to including the full GW vertex) and then taking the static limit for both terms. The resulting energy expression fulfills the crossing symmetry of the vertex to first order in the electron-electron interaction. Preliminary results for the correlation energies of atoms have been promising.¹¹⁹ This realization of SOSEX is computationally more efficient than AC-SOSEX since no expensive numerical frequency integration is required. Here, we compare the performance of this method to RPA and RPA+AC-SOSEX for non-covalent interactions for the S66 and S66x8 test sets.¹²¹ Our results show that, independently of the choice of the input KS Green's function, both RPA+SOSEX variants consistently outperform RPA and that the statically screened SOSEX variant is comparable in accuracy to AC-SOSEX.

The remainder of this work is organized as follows. In section 2 we give a detailed derivation of the different SOSEX energy expressions starting directly from MBPT. After an outline of our computational approach and implementation in section 3, we present and analyze our results for non-covalent interaction energies in section 4. Finally, section 5 summarizes and concludes this work.

2 Theory

Within MBPT, the electron-electron interaction energy can be obtained as²⁷

$$\begin{aligned}
 E_{Hxc}[G] &= E_{Hx}[G] + E_c[G] \\
 E_{Hx}[G] &= \frac{1}{2} \int d1d2 G(1, 2) \Sigma_{Hxc}^{(1)}(2, 1)[G] \\
 E_c[G] &= \frac{1}{2} \sum_{n=2} \frac{1}{n} \int d1d2 G(1, 2) \Sigma_{Hxc}^{(n)}(2, 1)[G] ,
 \end{aligned} \tag{1}$$

where Σ_{Hxc} is the one-particle irreducible (1PI) electronic self-energy. It is the sum of all 1PI skeleton diagrams (diagrams which do not contain any self-energy insertions) of n th order in the electron-electron interaction v_c . Space, spin, and imaginary time indices are collected as $1 = (\mathbf{r}_1, \sigma_1, i\tau_1)$. One can always switch between imaginary time and imaginary frequency using the Laplace transforms¹²²

$$f(i\tau) = \frac{i}{2\pi} \int d\omega F(i\omega) e^{i\omega\tau} \quad (2)$$

and

$$f(i\omega) = -i \int d\tau F(i\tau) e^{-i\omega\tau} . \quad (3)$$

Σ is a functional of the single-particle Green's function $G = G_1$, which in turn depends on the 2-particle Green's function G_2 . These quantities are defined by

$$G_n(1, \dots, 2n) = \left\langle \Psi_0^{(N)} \left| \mathcal{T} \left[\hat{\psi}^\dagger(1) \hat{\psi}(2) \dots \hat{\psi}^\dagger(2n-1) \hat{\psi}(2n) \right] \right| \Psi_0^{(N)} \right\rangle . \quad (4)$$

Here, $\Psi_0^{(N)}$ is the ground state of an N -electron system, \mathcal{T} is the time-ordering operator and $\hat{\psi}$ is the field operator. The self-energy maps G to its non-interacting counterpart $G^{(0)}$ by means of Dyson's equation,¹²³

$$G(1, 2) = G^{(0)}(1, 2) + G^{(0)}(1, 3) \Sigma(3, 4) G(4, 2) . \quad (5)$$

The exchange-correlation (xc) contribution to it can be written compactly as

$$\Sigma_{xc}(1, 2) = iG(1, 2)W(1, 2) + iG(1, 3)W(1, 4)\chi^{(0)}(6, 4, 5, 4^+)\Gamma_{xc}^{(0)}(6, 5, 2, 3) . \quad (6)$$

The quantities appearing in (6) are the particle-hole irreducible 4-point vertex (i.e. the sum of all diagrams which can not be cut into parts by removing a particle and a hole line),¹²⁴

$$\Gamma_{Hxc}^{(0)}(1, 2, 3, 4) = \Gamma_H^{(0)}(1, 2, 3, 4) + \Gamma_{xc}^{(0)}(1, 2, 3, 4) = i \frac{\delta \Sigma_H(1, 3)}{\delta G(4, 2)} + i \frac{\delta \Sigma_{xc}(1, 3)}{\delta G(4, 2)}, \quad (7)$$

the non-interacting generalized susceptibility,

$$\chi^{(0)}(1, 2, 3, 4) = -iG(1, 4)G(2, 3), \quad (8)$$

and the screened Coulomb interaction W , defined by

$$W(1, 2) = W^{(0)}(1, 2) + W^{(0)}(1, 3)P(3, 4)W^{(0)}(4, 2), \quad (9)$$

with

$$P(1, 2) = \int d3d4 \chi(1, 2, 3, 4) \delta(1, 4) \delta(2, 3), \quad (10)$$

and

$$W^{(0)}(1, 2) = v_c(\mathbf{r}_1, \mathbf{r}_2) \delta_{\sigma, \sigma'} \delta(t_1 - t_2), \quad (11)$$

given in terms of the bare coulomb interaction v_c . In equation (14), P is the reducible polarizability, which is the diagonal of the particle-hole reducible generalized susceptibility χ , defined by

$$\chi(1, 2, 3, 4) = -iG_2(1, 2, 3, 4) - iG(1, 2)G(3, 4). \quad (12)$$

It is related to it's non-interacting counterpart $\chi^{(0)}$ by a Bethe-Salpeter equation (BSE),^{124,125}

$$\chi(1, 2, 3, 4) = \chi^{(0)}(1, 2, 3, 4) + \chi^{(0)}(1, 8, 3, 7) \Gamma_{Hxc}^{(0)}(7, 5, 8, 6) \chi(6, 2, 5, 4), \quad (13)$$

which reduces to a Dyson equation for the polarizability P when the xc-contribution to the 4-point vertex is set to zero. One can then also introduce the irreducible polarizability $P^{(0)}$

as

$$P^{(0)}(1, 2) = \int d3d4\chi^{(0)}(1, 2, 3, 4)\delta(1, 4)\delta(2, 3) , \quad (14)$$

which is useful to define the RPA correlation energy. Using this quantity, (9) can also be written as

$$W(1, 2) = W^{(0)}(1, 2) + W^{(0)}(1, 3)P^{(0)}(3, 4)W(4, 2) . \quad (15)$$

When eqs. (5)–(10) and (13) are solved self-consistently, the expression for the correlation energy (1) becomes exact. Note, that the equations above are different from, but completely equivalent to Hedin’s equations.³² They have the advantage that the BSE appears explicitly, and also that only 2-point or 4-point quantities occur. The resulting equations are therefore invariant under unitary transformations of the basis, as has for instance been pointed out by Starke and Kresse.¹²⁶ or in ref. 127

In practice, eqs. (5)–(10) and (13) need to be truncated to obtain a closed system of equations. Setting $\Gamma_{xc}^{(0)} = 0$ defines the GWA. One typically also introduces a new non-interaction KS Green’s function G^s ,¹²⁸

$$G^s(1, 2) = G^{(0)}(1, 2) + G^{(0)}(1, 3)v_s(3, 4)G^s(4, 1) , \quad (16)$$

with

$$v_s(1, 2) = v_H(1, 2)\delta(1, 2) + v_{xc}(\mathbf{r}_1, \mathbf{r}_2)\delta(\tau_{12}) \quad (17)$$

where v_H is the Hartree-potential, v_{xc} is a KS xc-potential mixed with a fraction of HF exchange and $\tau_{12} = \tau_1 - \tau_2$, and evaluates (1) with G^s ,

$$E_c = \frac{1}{2} \sum_{n=2} \frac{1}{n} \int d1d2G^s(1, 2)\Sigma_{Hxc}^{(n)}(2, 1)[G^s] . \quad (18)$$

With the *GW* approximation for Σ and using (14) and (9),

$$\begin{aligned} E_{xc}^{RPA} &= i\frac{1}{2} \int d1d2 G^s(1,2)G(2,1)W(2,1) \\ &= -\frac{1}{2} \int d1d2 P^{(0)}(1,2) \left\{ W^{(0)}(1,2) + \frac{1}{2}W^{(0)}(1,3)P^{(0)}(3,4)W^{(0)}(4,2) + \dots \right\} \end{aligned} \quad (19)$$

is obtained. Isolating the exchange contribution to the Hartree-exchange energy,

$$E_x = \int d1d2 \delta(\tau_{12})G(1,2)W^{(0)}(2,1)G(2,1), \quad (20)$$

we obtain the RPA correlation energy

$$\begin{aligned} E_c^{RPA} &= -\frac{1}{2} \sum_n \frac{1}{n} \int d1d2 \left\{ \left[\int d3 P^{(0)}(1,3)W^{(0)}(3,2) \right]^n + \int d3 P^{(0)}(1,3)W^{(0)}(3,2) \right\} \\ &= \frac{1}{2} \int d1d2 \left\{ \ln \left[\delta(1,2) - \int d3 P^{(0)}(1,3)W^{(0)}(3,2) \right] + \int d3 P^{(0)}(1,3)W^{(0)}(3,2) \right\}, \end{aligned} \quad (21)$$

and using (2) as well as the symmetry of the polarizability on the imaginary frequency axis, its well-known representation due to Langreth and Perdew¹³ is obtained,

$$\begin{aligned} E_c^{RPA} &= \frac{1}{2\pi} \int d\mathbf{r}_1 d\mathbf{r}_2 \int_0^\infty d\omega \left\{ \ln \left[\delta(1,2) - \int d\mathbf{r}' P^{(0)}(\mathbf{r}_1, \mathbf{r}', i\omega) v_c(\mathbf{r}', \mathbf{r}_2) \right] \right. \\ &\quad \left. + \int d\mathbf{r}' P^{(0)}(\mathbf{r}_1, \mathbf{r}', i\omega) v_c(\mathbf{r}', \mathbf{r}_2) \right\}. \end{aligned} \quad (22)$$

In this work, we are interested in approximations to the self-energy beyond the GWA. From the antisymmetry of Fermionic Fock space, it follows that G_2 needs to change sign when the two creation or annihilation operators in (4) are interchanged. This property is known as crossing symmetry.¹²⁹ In the RPA, the crossing symmetry is violated which leads to the well-known overestimation of absolute correlation energies. One can show (see ref. 129 or ref. 130 for details) that the crossing symmetry of G translates into the requirement

$$\frac{\delta\Sigma(1,3)}{\delta G(4,2)} \stackrel{!}{=} \frac{\delta\Sigma(1,4)}{\delta G(3,2)}, \quad (23)$$

for the 4-point vertex. In the GWA, the irreducible vertex is approximated with the Hartree-vertex,¹³¹

$$\Gamma_{Hxc}^{(0)}(1, 2, 3, 4) \approx \Gamma_H^{(0)}(1, 2, 3, 4) = -i \frac{1}{\delta G(1, 3)} \delta(1, 3) \int d2 W^{(0)}(1, 2) G(2, 2^+) . \quad (24)$$

We then obtain

$$\begin{aligned} \frac{\delta \Sigma_H(1, 3)}{\delta G(4, 2)} &= -i \delta(1, 3) \delta(2, 4) v_c(1, 2) \\ \frac{\delta \Sigma_H(1, 4)}{\delta G(3, 2)} &= -i \delta(1, 4) \delta(2, 3) v_c(1, 2) , \end{aligned} \quad (25)$$

and therefore (23) is violated. When the 4-point vertex is approximated by the functional derivative of the Hartree-exchange self-energy, we obtain

$$\frac{\delta \Sigma_{Hx}(1, 3)}{\delta G(4, 2)} = -i v_c(1, 2) [\delta(1, 3) \delta(2, 4) - \delta(1, 4) \delta(2, 3)] = \frac{\delta \Sigma_{Hx}(1, 4)}{\delta G(3, 2)} , \quad (26)$$

i.e. the crossing symmetry is fulfilled. Approximations to the self-energy in Hedin's equations always violate the crossing symmetry.^{130,132} However, with each iteration of Hedin's pentagon, the crossing symmetry is fulfilled up to an increasingly higher order in v_c . We can then expect to obtain improvements over the RPA energies expressions by choosing a self-energy which fulfills the crossing symmetry to first order in v_c . The easiest approximation to the self-energy of this type is obtained from the HF vertex,

$$\Gamma_{xc}^{(0),HF}(1, 2, 3, 4) = i \frac{\delta \Sigma_{xc}^{HF}(1, 3)}{\delta G^s(4, 2)} = -W^{(0)}(1, 2) \delta(1, 4) \delta(3, 2) . \quad (27)$$

Using this expression in (6) with (8) yields the AC-SOSEX contribution to the self-energy,¹¹⁶

$$\Sigma^{\text{SOSEX}(W, v_c)}(1, 2) = - \int d3 d4 G^s(1, 3) W(1, 4) G^s(3, 4) G^s(4, 2) W^{(0)}(3, 2) , \quad (28)$$

where we have indicated the screening of the electron-electron interaction in the SOSEX expression in the superscript on the *l.h.s.* of (28). If one instead uses the *GW* self-energy

for $\Gamma^{(0)}$, the screened exchange kernel is obtained,

$$\Gamma_{xc}^{(0),GW}(1, 2, 3, 4) = i \frac{\delta \Sigma_{xc}^{GW}(1, 3)}{\delta G^s(4, 2)} = -W(1, 2)\delta(1, 4)\delta(3, 2) . \quad (29)$$

The resulting self-energy is the complete second-order term in the expansion of the self-energy in terms of the screened electron-electron interaction,³²

$$\Sigma^{G3W2}(1, 2) = - \int d3d4 G^s(1, 3)W(1, 4)G^s(3, 4)G^s(4, 2)W(3, 2) \quad (30)$$

and contains the AC-SOSEX self-energy. The $G3W2$ self-energy can be decomposed into eight skeleton diagrams on the Keldysh contour,¹³³ but the AC-SOSEX self-energy only into four.¹³⁴ In practice, the evaluation of the resulting energy expression requires to perform a double frequency integration while the evaluation of the AC-SOSEX energy only requires a single frequency integration. Since the computation of the AC-SOSEX term is already quite cumbersome, the complete $G3W2$ energy expression is therefore not a good candidate for an efficient beyond-RPA correction. Instead, we take the static limit in both W in (30) to arrive at a self-energy expression similar to AC-SOSEX,

$$\Sigma^{\text{SOSEX}(W^{(0)}, W^{(0)})}(1, 2) = - \int d3d4 G^s(1, 3)W(1, 4)G^s(3, 4)G^s(4, 2)W(3, 2)\delta(\tau_{32})\delta(\tau_{14}) . \quad (31)$$

This expression resembles the MP2 self-energy, with the difference that the bare electron-electron interaction is replaced by the statically screened one. The resulting expression for the correlation energy will be different in general due to the factors $\frac{1}{n}$ in (1). However, we will show in the following that the energy expression can be evaluated in exactly the same way as the MP2 energy when the sum over n is approximated in a suitable way. Using (9), eq. (31) can be written as

$$\Sigma^{\text{SOSEX}(W^{(0)}, W^{(0)})}(1, 2) = \Sigma^{\text{MP2-SOX}}(1, 2) + \Sigma^{\delta\text{MP2-SOX}}(1, 2) , \quad (32)$$

with the first term being the SOX term in MP2 and with the remainder accounting for the screening of the electron-electron interaction. Defining

$$\delta W(1, 2) = \int d3d4 W^{(0)}(1, 3) P(3, 4) W^{(0)}(4, 2) , \quad (33)$$

it can be written as

$$\Sigma^{\delta\text{MP2-SOX}}(1, 2) = - \int d3d4 G^s(1, 3) \delta W(1, 4) \delta(\tau_{14}) G^s(3, 4) G^s(4, 2) \delta W(3, 2) \delta(\tau_{32}) . \quad (34)$$

In the same way one can see, that the statically screened GW vertex contains the HF vertex. The same is obviously true for all other flavours of SOSEX, and therefore all of them fulfill the crossing symmetry of the full 4-point vertex to first order in the electron-electron interaction. Therefore, all of these approximations compensate the overestimation of the electron correlation energy in the RPA.

In contrast to the RPA which is efficiently evaluated in a localized basis, beyond-RPA energies are most easily formulated in the molecular spin-orbital basis $\{\phi_i(\mathbf{r}, \boldsymbol{\sigma})\}$ in which the time-ordered KS Green's function is diagonal,

$$\begin{aligned} G_{kk'}^s(i\tau_{12}) &= \delta_{kk'} \Theta(\tau_{12}) G_{kk'}^>(i\tau_{12}) - \delta_{kk'} \Theta(\tau_{21}) G_{kk'}^<(i\tau_{21}) \\ G_{kk}^>(i\tau_{12}) &= i(1 - f(\epsilon_k)) e^{-\epsilon_k \tau_{12}} \\ G_{kk}^<(i\tau_{12}) &= i f(\epsilon_k) e^{-\epsilon_k \tau_{12}} . \end{aligned} \quad (35)$$

The ϵ_k denote KS eigenvalues which are understood to be measured relative to the chemical potential μ and $f(\epsilon_k)$ denotes the occupation number of the k th orbital.

One can now obtain energy expressions analogous to (22). For example, inserting the

AC-SOSEX self-energy (28) into (18), we obtain

$$E_c^{\text{SOSEX}} = \frac{1}{2} \int d1d2d3d4 G^s(1,2)G^s(2,3)G^s(3,4)G^s(4,1) \\ \times \left\{ \frac{1}{2}W^{(0)}(3,1)W^{(0)}(2,4) + \frac{1}{3}W^{(0)}(3,1)W^{(0)}(2,5)P^{(0)}(5,6)W^{(0)}(6,4) + \dots \right\} . \quad (36)$$

In contrast to the RPA energy expression, the terms in this equations can not be summed exactly due to the presence of the $1/n$ -terms. However, defining

$$\Sigma_{Hxc}^\lambda = \sum_{n=1}^{\infty} \lambda^n \Sigma_{Hxc}^{(n)} [G^s, v_c] . \quad (37)$$

we can rewrite (18)

$$E_c = \frac{1}{2} \sum_{n=2}^{\infty} \frac{1}{n} \int d1d2 G^s(1,2) \Sigma_{Hxc}^{(n)}(2,1)[G^s] = \frac{1}{2} \int_0^1 \frac{d\lambda}{\lambda} \int d1d2 G^s(1,2) \Sigma_{Hxc}^{(\lambda)}(2,1)[G^s] , \quad (38)$$

as an integral over a coupling constant λ . We can now rewrite (37) as

$$\Sigma_{Hxc}^\lambda = \sum_{n=1}^{\infty} \Sigma_{Hxc}^{(n)} [G^s, \lambda v_c] = \sum_{n=1}^{\infty} \Sigma_{Hxc}^{(n)} [G^s, W^{(\lambda)}] , \quad (39)$$

where $W^{(\lambda)}$ is defined as in (15), with $W^{(0)}$ replaced by $\lambda W^{(0)}$. Defining

$$\bar{W} = \int_0^1 d\lambda W^{(\lambda)} , \quad (40)$$

and

$$\bar{\Sigma} = \Sigma [\bar{W}] \quad (41)$$

the correlation energy becomes

$$E_c = \frac{1}{2} \int d1d2 G^s(1,2) \bar{\Sigma}_c(2,1) . \quad (42)$$

The integral in (40) needs to be computed numerically, but converges typically very fast when Gauss-Legendre grids are employed.⁹² In ref. 135 a trapezoidal rule for the solution of this integral has been used and also ref. 5 suggests that this choice is often suitable for the calculation of correlation energies within the RPA and beyond. Below, we will assess the effect of such approximate coupling constant integration on absolute and relative correlation energies. Notice, that using a trapezoidal rule, (42) reduces to

$$E_c = \frac{1}{4} \int d1d2 G^s(1,2)\Sigma_c(2,1) , \quad (43)$$

and when the statically screened $G3W2$ self-energy (31) is used in this expression, the energy expression of ref. 119 is obtained. When additionally both $W(0)$ are replaced by $W^{(0)}$, (43) gives the MP2 correlation energy (evaluated with G^s).³¹ Therefore, the correlation energy expression obtained in this way can be interpreted as a renormalized variant of MP2.

Using (42), simple expressions for the AC-SOSEX energy in the canonical basis of KS orbitals can be obtained. With (42), the self-energy (28) and (35) we have

$$\begin{aligned} E^{\text{SOSEX}(W,v_c)} &= \frac{i}{2} \sum_{pqrs} \int d\tau_{12} d\tau_3 G_p^s(\tau_{13}) G_q^s(\tau_{31}) G_r^s(\tau_{12}) G_s^s(\tau_{21}) W_{spqr}^{(0)} \bar{W}_{rspq}(\tau_{23}) \\ &= -\frac{1}{4\pi} \sum_{pqrs} \int d\omega' W_{spqr}^{(0)} \bar{W}_{rspq}(i\omega') \int d\tau_{12} G_r^s(\tau_{12}) G_s^s(\tau_{21}) \\ &\quad \times \underbrace{\int d\tau_3 e^{-i\omega'\tau_{23}} G_p^s(\tau_{13}) G_q^s(\tau_{31})}_{I(i\tau_{12})} . \end{aligned} \quad (44)$$

In going from the second equations, we have used (2) to transform W to the imaginary frequency axis. The integral over τ_3 can be evaluated by splitting it at τ_1 and using the definition of the KS Green's function (35),

$$I(i\tau_{12}) = \frac{[(1-f(\epsilon_p))f(\epsilon_q) - (1-f(\epsilon_q))f(\epsilon_p)] e^{i\omega'\tau_{12}}}{\epsilon_p - \epsilon_q + i\omega'} = -e^{i\omega'\tau_{12}} \frac{f(\epsilon_p) - f(\epsilon_q)}{\epsilon_p - \epsilon_q + i\omega'} \quad (45)$$

The remaining integral over τ_{12} is

$$I_{\tau_{12}} = - \int G_r^{(0)}(\tau_{12}) G_s^{(0)}(\tau_{21}) e^{i\omega' \tau_{12}} d\tau_{12} = \frac{f(\epsilon_r) - f(\epsilon_s)}{\epsilon_r - \epsilon_s - i\omega'}, \quad (46)$$

so that the correlation energy becomes

$$E^{\text{SOSEX}(W, v_c)} = - \frac{1}{4\pi} \sum_{pqrs} \int d\omega' W_{spqr}^{(0)} \overline{W}_{rspq}(i\omega') \frac{f(\epsilon_r) - f(\epsilon_s)}{\epsilon_r - \epsilon_s - i\omega'} \frac{f(\epsilon_p) - f(\epsilon_q)}{\epsilon_p - \epsilon_q + i\omega'} \quad (47)$$

Each of the nominators can only give a non-vanishing contribution if one of the two occupation numbers is zero. If the difference of the occupation numbers is -1 , we simply flip sign in the denominator. Without loss of generality we can then decide that the indices r and p belong to occupied and the indices s and q to virtual single-particle states. This gives us a factor of 4. We can then use the symmetry of the Coulomb interaction and finally sum over spins (i.e. transforming to a basis of spatial orbitals), which gives an additional factor of 2. Therefore, we recover the well-known SOSEX correlation energy expression for a closed-shell system^{92,135} as

$$E^{\text{SOSEX}(W, v_c)} = - \frac{1}{2\pi} \sum_{ij}^{\text{occ}} \sum_{ab}^{\text{virt}} \int_0^\infty d\omega \overline{W}_{iajb}(i\omega) W_{jaib}^{(0)} \frac{4(\epsilon_i - \epsilon_a)(\epsilon_j - \epsilon_b)}{[(\epsilon_i - \epsilon_a)^2 + \omega^2][(\epsilon_j - \epsilon_b)^2 + \omega^2]}. \quad (48)$$

In a spatial orbital basis, the SOSEX($W(0)$, $W(0)$) Correlation energy is obtained from (30) and (35) as

$$\begin{aligned} E^{\text{SOSEX}(W(0), W(0))} &= - \frac{1}{2} \sum_{pqrs} \int d\tau_{12} G_p^s(\tau_{12}) G_q^s(\tau_{21}) G_r^s(\tau_{12}) G_s^s(\tau_{21}) \\ &\quad \times \overline{W}_{spqr}(i\omega = 0) \overline{W}_{rspq}(i\omega = 0) \\ &= - \sum_{ij}^{\text{occ}} \sum_{ab}^{\text{virt}} \frac{\overline{W}_{spqr}(i\omega = 0) \overline{W}_{rspq}(i\omega = 0)}{\epsilon_i + \epsilon_j - \epsilon_a - \epsilon_b}. \end{aligned} \quad (49)$$

This is the expression we have introduced in ref. 119. It is completely equivalent to the

exchange term in MP2 with the bare electron-electron interaction replaced by the statically screened, coupling constant averaged one. Both RPA+SOSEX variants can be understood as renormalized MP2 expressions and have a clear diagrammatic interpretation. In the next section, we briefly outline our implementation of these expressions, before we proceed by assessing their accuracy for non-covalent interactions in sec. 4.

3 Technical and Computational Details

All expressions presented herein have been implemented in a locally modified development version of the Amsterdam density functional (ADF) engine of the Amsterdam modelling suite 2022 (AMS2022).¹³⁶ The non-interacting polarizability needed to evaluate (22) and (15) is calculated in imaginary time with quadratic scaling with system size in the atomic orbital basis. The implementation is described in detail in ref. 43. In all calculations, we expand the KS Green’s functions in correlation consistent bases of Slater-type orbitals of triple- and quadruple- ζ quality (TZ3P and QZ6P, respectively).¹³⁷ All 4-point correlation functions (screened and unscreened Coulomb interactions as well as polarizabilities) are expressed in auxiliary basis sets of Slater type functions which are usually 5 to 10 times larger than the primary bases. In all calculations, we use auxiliary basis sets of *VeryGood* quality. The transformation between primary and auxiliary basis (for the polarizability) is implemented with quadratic scaling with system size using the pair-atomic density fitting (PADF) method for products of atomic orbitals.^{138,139} For an outline of the implementation of this method in ADF, we refer to ref. 140. Eq. (22) is then evaluated in the basis of auxiliary fit functions with cubic scaling with system size. Eqs. (48) and (49) are evaluated with quintic scaling with system size in the canonical basis of KS states. This implementation is completely equivalent to the canonical MP2 implementation outlined in ref. 140. Eq. (40) is evaluated using small Gauss-Legendre grids. In case of a single λ -point, a trapezoidal rule is used for integration.

Imaginary time and imaginary frequency variables are discretized using non-uniform bases

$\mathcal{T} = \{\tau_\alpha\}_{\alpha=1,\dots,N_\tau}$ and $\mathcal{W} = \{\omega_\alpha\}_{\alpha=1,\dots,N_\omega}$ of sizes N_τ and N_ω , respectively, tailored to each system. More precisely, (2) and (3) are then implemented by splitting them into sine- and cosine transformation parts as

$$\begin{aligned}\overline{F}(i\omega_\alpha) &= \sum_{\beta} \Omega_{\alpha\beta}^{(c)} \overline{F}(i\tau_\beta) \\ \underline{F}(i\omega_\alpha) &= \sum_{\beta} \Omega_{\alpha\beta}^{(s)} \underline{F}(i\tau_\beta),\end{aligned}\tag{50}$$

where \overline{F} and \underline{F} denote even and odd parts of F , respectively. The transformation from imaginary frequency to imaginary time only requires the (pseudo)inversion of $\Omega^{(c)}$ and $\Omega^{(s)}$, respectively. Our procedure to calculate $\Omega^{(c)}$ and $\Omega^{(s)}$ as well as \mathcal{T} and \mathcal{W} follows Kresse and coworkers.^{141–143} The technical specifications of our implementation have been described in the appendix of ref. 137.

We use in all calculations grids of 24 points in imaginary time and imaginary frequency which is more than sufficient for convergence.¹⁴⁰ The final correlation energies are then extrapolated to the complete basis set limit using the relation,¹⁴⁴

$$E_{CBS} = E_{QZ} + \frac{E_{QZ} * 4^3 - E_{TZ} * 3^3}{4^3 - 3^3},\tag{51}$$

where E_{QZ} (E_{TZ}) denotes the total energies at the QZ6P (TZ3P) level. The extrapolation scheme has been shown to be suitable for correlation consistent basis sets but can not be used for KS or HF contributions.^{144,145} Therefore, we do not extrapolate the DFT energies, but assume them to be converged on the QZ level. Since the basis set error is not completely eliminated with this approach, we also counterpoise correct all energies, taking into account 100 % of the counterpoise correction. With these settings, we assume all our calculated values to be converged well enough to be able to draw quantitative conclusions about the performance of the methods we benchmark herein. We use the *VeryGood* numerical quality for integrals over real space and distance cut-offs. Dependency thresholds⁴³ have been set

to $5e^{-4}$.

4 Results

Dependence on the λ -Integration

We now assess the accuracy of the post-RPA approaches for the S66 database and first discuss the dependence of the SOSEX correlation energies on the λ -integration. The magnitude of the SOSEX contribution to the correlation energy as a function of the size of the λ -grid is shown in table 1 for three selected systems. One can show, that for a 2-electron system like H_2 , the $\text{SOSEX}(W, v_c)$ correction equals minus half of the RPA correlation energy (In other words, RPA+SOSEX is self-correlation free). This relation is fulfilled for $\text{SOSEX}(W, v_c)$ with already 4 Gauss-Legendre points. The magnitude of the SOSEX correction is underestimated when the λ -integration is carried out using a trapezoidal rule. This is illustrated in fig. 1 for H_2 and $(\text{H}_2\text{O})_2$. Using a single-frequency point corresponds to approximating the λ -dependence of the correlation energy as a straight line, which leads to a small integration error.

Table 1: Total magnitude of SOSEX correction in kcal/mol as a function of the size of the λ -grid for selected systems.

N_λ	SOSEX(W, v_c)			SOSEX($W(0), W(0)$)		
	H_2	$(\text{H}_2\text{O})_2$	Benzene	H_2	$(\text{H}_2\text{O})_2$	Benzene
1	15.51400	147.15253	287.90735	10.74228	101.45448	204.17377
2	16.63810	157.79684	307.48549	12.83037	119.99186	239.22546
4	16.63421	157.71007	307.35326	12.82006	119.79484	238.91728
6	16.63421	157.70997	307.35313	12.82006	119.79451	238.91688
$\frac{1}{2}E^{RPA}$	16.63421			16.63421		

Let us now look at the effect on relative energies for $\text{SOSEX}(W, v_c)$ and $\text{SOSEX}(W, W(0))$. For the S66 test set, the results of this comparison is shown in figure 2. Fig. 2 a) shows the error in the covalent bonding energies with respect to the converged λ -integration when

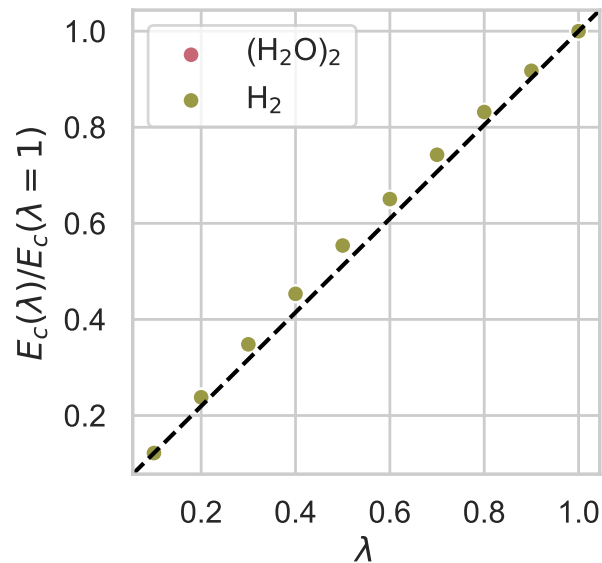


Figure 1: Magnitude of the SOSEX(W, v_c) correlation energy as a function of λ relative to its value at $\lambda = 1$ for H_2 and $(\text{H}_2\text{O})_2$.

only a single integration point is used. Generally, the resulting integration errors are very small and do not exceed 0.1 kcal/mol for most complexes. In parts b) and c) of figure 2, the relative errors of the interaction energies with respect to the CCSD(T) reference values are shown. One can clearly see, that the error in the λ -integration is negligible when looking at the accuracy of relative energies. This is also reflected in the MADs with respect to the CCSD(T) reference shown in figure 2.

Dependence on the KS Green's function

We next discuss the dependence of the correlation energies on the choice of the KS Green's function G^s . RPA calculations can in principle be performed self-consistently using a variety of approaches^{93,146–153} (see ref. 154 for a review) but this is rarely done in practice. For once, self-consistent RPA calculations are computationally demanding. Furthermore, the resulting energies are often worse than the ones evaluated using a Green's function from a generalized gradient approximation (GGA) or hybrid calculation.¹⁴⁸ GGAs like PBE or TPSS are often used to construct G^s .^{11,55,92} However, for GW calculations it is well known

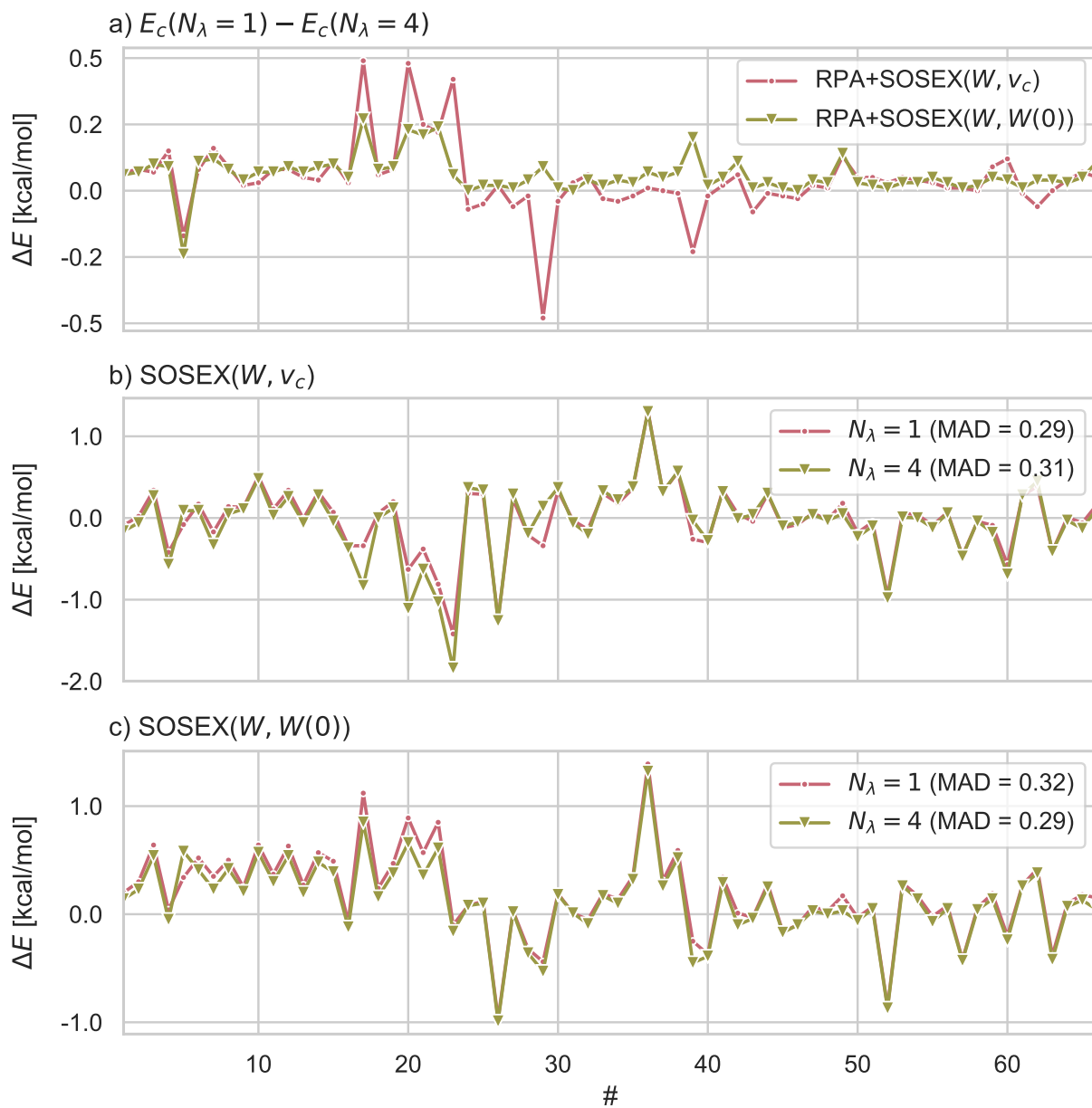


Figure 2: a) Difference in relative correlation energies for the S66 test set for both SOSEX variants when using 1 and 4 integration points for the λ -integration. b) Error of relative SOSEX(W, v_c) correlation energies with respect to the CCSD(T) reference values when using 1 and 4 integration points for the λ -integration. c) Same as b), but for SOSEX($W, W(0)$). All values are in kcal/mol.

that GGAs produce a much too low band gap and therefore the screening within the bubble approximation is massively overestimated.⁶⁵ Hybrid functional with 25 - 50 % exact exchange are always a much better choice.¹⁵⁵ The situation is similar for RPA calculations.⁵⁴

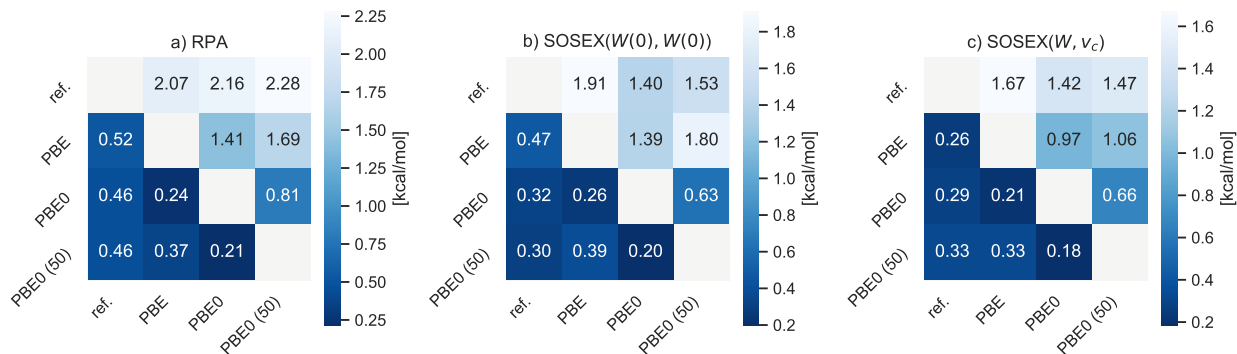


Figure 3: Mean absolute deviations (MAD) (lower triangle in each plot) and Maximum deviations (MAX) (upper triangle) for a) RPA, b) SOSEX($W(0), W(0)$) and c) SOSEX($W(0), v_c$) interaction energies for the S66 database using different KS Green's functions as well as to the CCSD(T) reference values (ref.). All values are in kcal/mol.

In figure 3, mean absolute deviations (MAD) and maximum deviations (MAX) are shown for the S66 database for RPA and SOSEX($W(0), W(0)$). All values have been obtained using a single integration point for the λ -integral. The interaction energies obtained using the different Green's functions are compared to each other as well as to the CCSD(T) reference values by Hobza and coworkers.¹²¹ RPA and RPA+SOSEX($W(0), W(0)$) are more or less equivalently independent of the choice of the KS Green's function, with MADs between 0.20 and 0.39 kcal/mol between the different functionals. However, individual values can differ by almost 2 kcal/mol which is a sizable difference, given that the largest interaction energies in the S66 database are of the order of 20 kcal/mol only. The performance of RPA compared to the CCSD(T) reference is rather insensitive to the KS Green's function, even though the hybrid functionals perform slightly better. With 0.52 kcal/mol, the MAD for RPA@PBE is in excellent agreement with the 0.61 kcal/mol MAD obtained by Nguyen *et. al.* in ref. 55, which has been obtained with GTO-type basis sets and 50 % counterpoise correction instead of 100 %. This shows, that our interaction energies are well converged with respect to the basis set size. Also note, that the SOSEX contributions are expected to converge faster with respect to the basis size than the RPA contributions.¹⁵⁶ The SOSEX($W(0), W(0)$) results are much better using the hybrid functionals than with PBE. SOSEX(W, v_c), is slightly more accurate using the PBE Green's function than the PBE0 and PBE0(50) ones, but the

differences between the different starting points are negligibly small. Also, the dependence of $\text{SOSEX}(W, v_c)$ on the starting point is smaller than for $\text{SOSEX}(W(0), W(0))$. Independently of the choice of G^s , RPA+SOSEX always outperforms RPA.

S66 Interaction Energy

We now compare the accuracy of the different SOSEX corrections for the S66 database in more detail. The interactions of the first 22 complexes in the database are dominated by Hydrogen bonds, while the next 22 complexes are mostly bound by dispersion interactions. The remaining interactions are of mixed nature.¹²¹ It is therefore useful to distinguish between these different interaction patterns in the following comparison.

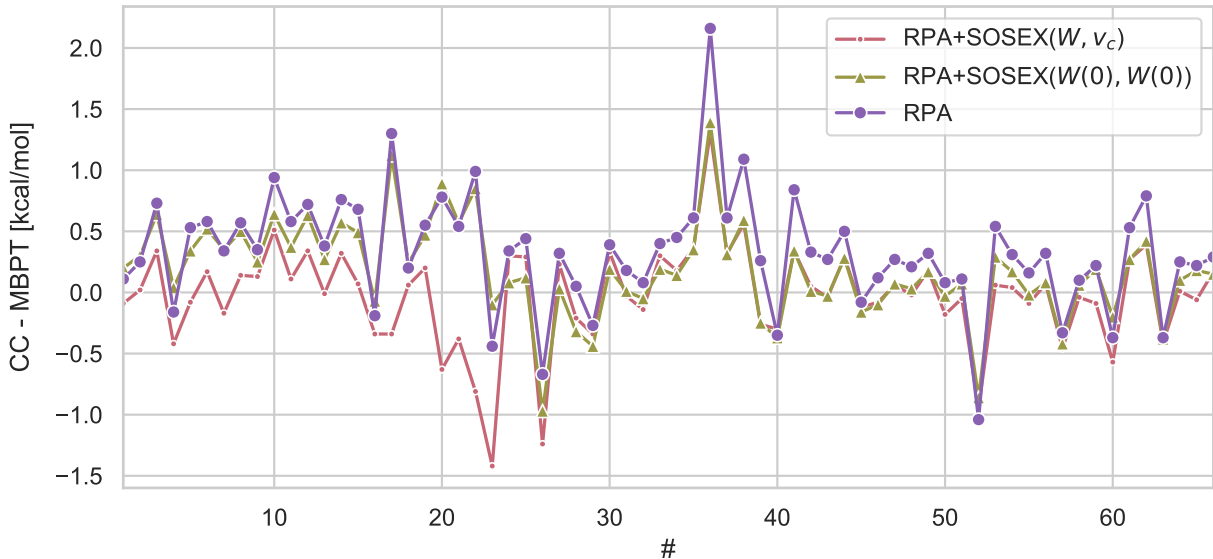


Figure 4: Deviations of RPA@PBE0 and both RPA + SOSEX@PBE0 variants for the S66 database with respect to the CCSD(T) reference. All values are in kcal/mol.

Figure 4 shows the deviations of RPA and both RPA+SOSEX variants with respect to CCSD(T) for all datapoints. MADs for the whole database and MADs given in percent of the CCSD(T) interaction energies for the whole database as well as for the individual categories are presented in table 2. For the whole database, RPA gives a MAD of 11.5 %. Both SOSEX corrections lead to a considerable improvement, reducing the MAD to in between 7.3 % and

Table 2: MADs (absolute and in %) of different electronic structure methods with respect to the CCSD(T) reference values for the whole S66 database and for its subcategories.

Method	MAD							
	S66		hydr. bond		dispersion		mixed	
	$[\frac{kcal}{mol}]$	[%]	$[\frac{kcal}{mol}]$	[%]	$[\frac{kcal}{mol}]$	[%]	$[\frac{kcal}{mol}]$	[%]
SOSEX($W(0), W(0)$)@PBE0	0.32	7.28	0.45	5.76	0.29	10.33	0.21	5.50
SOSEX(W, v_c)@PBE0	0.29	6.85	0.31	3.39	0.33	11.63	0.21	5.33
SOSEX(W, v_c)@PBE	0.26	6.25	0.23	3.51	0.33	10.16	0.17	4.26
RPA	0.46	11.54	0.55	7.19	0.47	17.74	0.34	9.41
PBE0-D3(BJ)	0.28	5.09	0.47	4.80	0.18	5.09	0.18	5.42
DSD-PBE-P86-D3(BJ)	0.23	5.07	0.31	3.71	0.21	6.99	0.16	4.43

6.3 %, depending on the starting point. SOSEX(W, v_c) outperforms SOSEX($W(0), W(0)$) by far for the hydrogen-bonded complexes, and is even slightly more accurate than the double-hybrid DSD-PBE-P86-D3(BJ),¹⁵⁷ one of the best double hybrid functionals for weak interactions.¹⁵⁸ For dispersion interactions, the performance of SOSEX($W(0), W(0)$) and SOSEX(W, v_c) is comparable. Here, the empirically dispersion corrected^{159,160} functionals, the hybrid PBE0-D3(BJ) and DSD-PBE-P86-D3(BJ), are much more accurate than all MBPT based methods. A few exceptions aside, fig. 4 shows that RPA overestimates the non-covalent interaction energies in the S66 database. SOSEX corrections lower the interaction energies, i.e. the non-covalently bound complexes become more stable. SOSEX(W, v_c) shows a tendency to overstabilize the hydrogen-bonded complexes. For these systems, the RPA+SOSEX($W(0), W(0)$) energies are almost identical to the ones from RPA.

Overall, SOSEX leads to significant improvements over RPA, making RPA+SOSEX competitive with dispersion corrected hybrid functionals, albeit their description of dispersion interactions is certainly inferior. An important observation is, that the dynamically screened SOSEX does not lead to an improved description of these effects compared to the statically screened one. This can be linked to the fact that the frequency dependence of the screening tends to be dominated by its static limit with increasing electron-electron separation. When the electron correlation effects are dominated by long-ranged interactions, the frequency-dependence of the screening therefore becomes unimportant. We will comment on this

observation in more detail below.

S66x8 Interaction Energy

We now assess the accuracy of these methods for the S66x8 dataset which contains the complexes in the S66 database at 8 different geometries.¹²¹ The separations of the monomers in the complexes are given relative to their equilibrium distances, i.e. a relative separation of 2.0 means that the monomers separation in the complex is twice as large as the equilibrium separation. For our assessment of the different SOSEX corrections, we divide the regions on the potential energy curve in three regions, which we denote as short (equilibrium distance scaled by a factor 0.9-0.95), middle (1.0-1.25) and long (1.5-2.0). All RPA (+SOSEX) calculation discussed here have been performed using a PBE0 Green’s function.

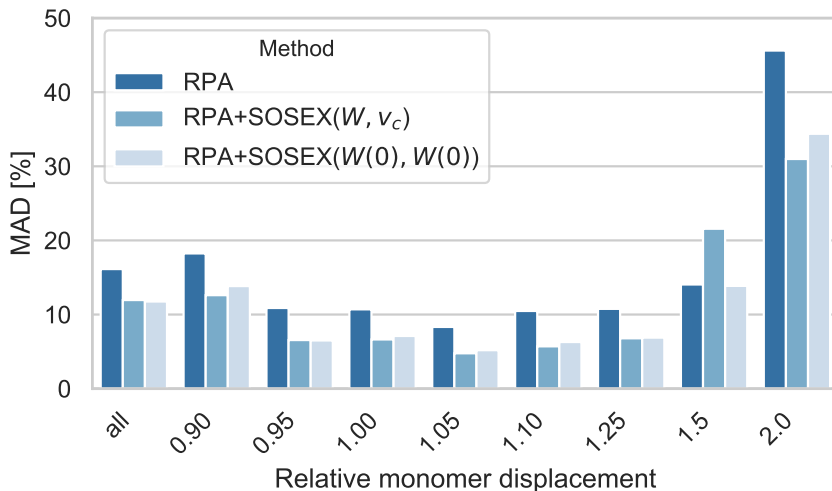


Figure 5: MADs (in percent) for the S66x8 database with respect to the CCSD(T) reference values for RPA, RPA+SOSEX(W, v_c) and RPA+SOSEX($W(0), W(0)$). MADs are shown separately for the whole database (columns on the left) and for different monomer-monomer separations.

The results of our comparison are shown in figure 5, where the MADs (given in percent) with respect to CCSD(T) for the whole database as well as for the scaled monomer-monomer separations are shown. For the whole database, the average relative deviations with respect to the reference values are larger than for S66. For once, this is due to the geometries

with large monomer-monomer separation for which the interaction energies are very small leading also to much larger relative errors. It is important to notice that with smaller interaction energies the relative importance of basis set expansion errors increases as well. However, also at short monomer-monomer separations, the relative errors increase slightly compared to the intermediate regime. This can probably be attributed to stronger electron correlation and screening effects at short monomer separations. As already alluded to in the introduction, with decreasing electron-electron distances vertex corrections in the electronic self-energy become more and more important and an expansion of the self-energy in terms of the screened electron-electron interaction will converge slower. Another factor might be, that screening effects beyond the bubble approximation might become more relevant.

Table 3: Relative improvements obtained with different SOSEX variants over RPA for different groups of monomer-monomer separations.

	short [%]	middle [%]	long [%]
SOSEX(W, v_c)	35.2	42.8	13.5
SOSEX($W(0), W(0)$)	31.0	37.9	19.1

We can make two interesting observations: First, in the short and medium regime, both SOSEX correction lead to sizable improvements over the RPA with in between 31 and 43 %. This is comparable to the observation for S66. For large monomer-monomer separations, the improvements become much smaller, with 14 % for SOSEX(W, v_c) and 19 % for SOSEX($W(0), W(0)$). Second, while at the equilibrium geometries SOSEX(W, v_c) shows a tendency to lead to larger improvements over the RPA than SOSEX($W(0), W(0)$), this is not longer true for large monomer separations.

The second point can be rationalized by the fact that at large electron-electron distances the frequency dependence of the screening averages out.²³ The first point can be related to the second Ward identity for the 4-point vertex.¹⁶¹ At large monomer-monomer separation, the interaction energies are dominated by long-range correlation effects. Following the argument by Kotani, van Schilfhaarde and Faleev,¹⁶² the interacting Green's function can be written

as

$$G = ZG^{(0)} + \bar{G} . \quad (52)$$

Here, $G^{(0)}$ is to be understood as the QP part of the interacting G (in our case, this is the KS Green's function), while the incoherent part \bar{G} contains all contributions which are not described within the independent-particle approximation. We can rewrite (6) as

$$\Sigma = GWI , \quad (53)$$

where $I = 1 - \Gamma_{xc}^{(0)}$. In the limit of large electron-electron separation and zero momentum transfer, it goes as

$$I \rightarrow 1 - \frac{\delta\Sigma}{\delta\omega} = \frac{1}{Z} \quad (54)$$

due to the second Ward identity.^{65,163,164} If we now assume that only this limit is important for the description of electron-electron correlation, we obtain

$$\Sigma = G^{(s)}W + \frac{1}{z}\bar{G}W . \quad (55)$$

We now need to assume that \bar{G} does not contribute to the total correlation energy at large electron-electron distances. Under this assumption, the correlation energy reduces to the RPA form. Note, that a similar argument also holds for the kernel of (13) in the long-range and low-frequency limit.¹⁶² In practice, we can neither ignore the short-range contributions to the correlation energy nor the incoherent part of the Green's function completely. However, this argument gives some indication as to why SOSEX hardly leads to any improvements over the RPA for large monomer separations. Other technical reasons certainly play a role as well. For instance, the importance of basis set errors will increase, since the magnitude of the interaction energy decreases.

5 Conclusions

The accuracy of the RPA can in principle be improved by including vertex correction in the self-energy. This can be done either directly, or indirectly through the solution of the BSE. In this work, we have assessed the accuracy of two closely related SOSEX corrections to RPA correlation energies for weak interactions. These are the well-known AC-SOSEX, herein termed $\text{SOSEX}(W, v_c)$, first introduced by Jansen *et. al.*,¹¹⁶ as well as an energy expression which is obtained from the statically screened $G3W2$ correction to the GW self-energy.^{119,120} This energy expression has already been introduced in ref. 119, albeit without a rigorous derivation. Especially, we have implicitly assumed that the integral over the coupling strength is evaluated using a trapezoidal rule. Here, we have introduced this expression (referred to as $\text{SOSEX}(W(0), W(0))$ in this work) with its proper λ -dependence.

We have then assessed the accuracy of these approximations for the S66 and S66x8 database of non-covalently bound complexes. Independently of the input KS Green’s function, both SOSEX corrections lead to significant improvements over RPA. Also, we have shown here that the coupling constant integration can be approximated by a trapezoidal rule without relevant loss of accuracy. Notice, that in implementations using DF, the evaluation of all λ -dependent terms only scales as N^3 . However, in implementations without DF such steps generally scale as N^6 and therefore evaluating the coupling-constant integration with a single frequency point results in substantial computational savings.¹⁶⁵

$\text{SOSEX}(W, v_c)$ is most accurate for the hydrogen-bonded complexes while $\text{SOSEX}(W(0), W(0))$ is slightly more accurate for dispersion interactions, indicating that the frequency-dependence of the screened interactions does not seem to be an important factor here. Our results for the S66x8 database revealed, that the improvements over RPA are largest for the non-covalently bounded complexes at their equilibrium distances. For large monomer-monomer separations, we have argued that this can be attributed to the Z -factor cancellation¹⁶² which is a consequence of the second Ward identity.^{161,163} Also, in the long-range limit, the differences between static and dynamic screening vanishes. While for equilibrium dis-

tances $\text{SOSEX}(W, v_c)$ is slightly more accurate than $\text{SOSEX}(W(0), W(0))$, this is not longer true for large monomer-monomer separations. A systematic assessment of the accuracy of RPA+SOSEX for a wider range of reaction types is currently missing. Especially for processes like bond breaking or ionization for which RPA is known to perform poorly,^{6,9} RPA+SOSEX approaches might be a promising alternative.

$\text{SOSEX}(W, v_c)$ and $\text{SOSEX}(W(0), W(0))$ both formally scale as N^5 with system size. While the computation of the $\text{SOSEX}(W, v_c)$ correction requires an a numerical integration over imaginary frequency, the $\text{SOSEX}(W(0), W(0))$ correction comes with the same computational cost as the evaluation of the SOX contribution to MP2. However, MP2 is inadequate for large molecules since it neglects screening effects entirely.^{1,55} In $\text{SOSEX}(W(0), W(0))$, the electron-electron interaction is screened and therefore RPA+SOSEX($W(0), W(0)$) is in principle applicable to large molecules. A stochastic linear scaling implementation of the SOSEX self-energy has already been developed.¹⁶⁶ Low-scaling MP2 implementations^{167–169} could potentially be generalized to SOSEX as well.

While the addition of SOSEX leads to significant improvements over the RPA for the description of dispersion interactions, RPA+SOSEX falls short of the accuracy of dispersion corrected hybrid or double hybrids. Going to higher orders in the expansion of the self-energy in terms of W might make MBPT based energy expressions competitive to these functionals. This would lead to at least an N^6 scaling with system size N . Augmenting the 4-point vertex in the BSE with additional non-local contributions leads to the same unfavourable scaling. It should be noted that faster algorithms for solving the BSE with these kernels have been proposed as well, but so far only for the calculation of polarizabilities.¹⁷⁰ It might therefore be a better solution to add local terms to the Hartree-kernel instead. Such modifications have recently been shown to lead to major improvements over the RPA for the description of dispersion interactions,¹⁰⁶ and their combination with SOSEX might result in even better accuracy.

Acknowledgement

This research received funding (project number 731.017.417) from the Netherlands Organisation for Scientific Research (NWO) in the framework of the Innovation Fund for Chemistry and from the Ministry of Economic Affairs in the framework of the “TKI/PPS-Toeslageregeling”. We thank Mauricio Rodríguez-Mayorga for fruitful discussions.

Supporting Information Available

.csv files with all calculated total energies and non-covalent interaction energies at the extrapolated CBS TZ3P, and QZ6P level. PDF with explanations

References

- (1) Macke, W. Über die Wechselwirkungen im Fermi-Gas. *Zeitschrift für Naturforsch.* **1950**, *5*, 192–208.
- (2) Bohm, D.; Pines, D. A collective description of electron interactions: III. Coulomb interactions in a degenerate electron gas. *Phys. Rev.* **1953**, *92*, 609–625.
- (3) Furche, F. Molecular tests of the random phase approximation to the exchange-correlation energy functional. *Phys. Rev. B - Condens. Matter Mater. Phys.* **2001**, *64*, 1–8.
- (4) Furche, F. Developing the random phase approximation into a practical post-Kohn-Sham correlation model. *J. Chem. Phys.* **2008**, *129*, 114105.
- (5) Heßelmann, A.; Görling, A. Random-phase approximation correlation methods for molecules and solids. *Mol. Phys.* **2011**, *109*, 2473–2500.

- (6) Eshuis, H.; Bates, J. E.; Furche, F. Electron correlation methods based on the random phase approximation. *Theor. Chem. Acc.* **2012**, *131*.
- (7) Ren, X.; Rinke, P.; Joas, C.; Scheffler, M. Random-phase approximation and its applications in computational chemistry and materials science. *J. Mater. Sci.* **2012**, *47*, 7447–7471.
- (8) Paier, J.; Ren, X.; Rinke, P.; Scuseria, G. E.; Grüneis, A.; Kresse, G.; Scheffler, M. Assessment of correlation energies based on the random-phase approximation. *New J. Phys.* **2012**, *14*, 043002.
- (9) Chen, G. P.; Voora, V. K.; Agee, M. M.; Balasubramani, S. G.; Furche, F. Random-Phase Approximation Methods. *Annu. Rev. Phys. Chem.* **2017**, *68*, 421–445.
- (10) Chedid, J.; Ferrara, N. M.; Eshuis, H. Describing transition metal homogeneous catalysis using the random phase approximation. *Theor. Chem. Acc.* **2018**, *137*, 1–11.
- (11) Kreppel, A.; Graf, D.; Laqua, H.; Ochsenfeld, C. Range-Separated Density-Functional Theory in Combination with the Random Phase Approximation: An Accuracy Benchmark. *J. Chem. Theory Comput.* **2020**, *16*, 2985–2994.
- (12) Langreth, D. C.; Perdew, J. P. The Exchange-Correlation Energy of a metallic surface. *Solid State Commun.* **1975**, *17*, 1425–1429.
- (13) Langreth, D. C.; Perdew, J. P. Exchange-correlation energy of a metallic surface: Wave-vector analysis. *Phys. Rev. B* **1977**, *15*, 2884–2901.
- (14) Harris, J.; Griffin, A. Correlation energy and van der Waals interaction of coupled metal films. *Phys. Rev. B* **1975**, *11*, 3669–3677.
- (15) Coester, F. Bound states of a many-particle system. *Nucl. Phys.* **1958**, *7*, 421–424.
- (16) Coester, F.; Kümmel, H. Short-range correlations in nuclear wave functions. *Nucl. Phys.* **1960**, *17*, 477–485.

- (17) Čížek, J. On the Correlation Problem in Atomic and Molecular Systems. Calculation of Wavefunction Components in Ursell-Type Expansion Using Quantum-Field Theoretical Methods. *J. Chem. Phys.* **1966**, *45*, 4256–4266.
- (18) Čížek, J. On the Use of the Cluster Expansion and the Technique of Diagrams in Calculations of Correlation Effects in Atoms and Molecules. *Adv. Chem. Physics, Vol. XIV* **1969**, *XIV*, 35–89.
- (19) Paldus, J.; Čížek, J.; Shavitt, I. Correlation Problems in Atomic and Molecular Systems. IV. Extended Coupled-Pair Many-Electron Theory and Its Application to the BH3 Molecule. *Phys. Rev. A* **1972**, *5*, 50–67.
- (20) Scuseria, G. E.; Henderson, T. M.; Sorensen, D. C. The ground state correlation energy of the random phase approximation from a ring coupled cluster doubles approach. *J. Chem. Phys.* **2008**, *129*, 231101.
- (21) Scuseria, G. E.; Henderson, T. M.; Bulik, I. W. Particle-particle and quasiparticle random phase approximations: Connections to coupled cluster theory. *J. Chem. Phys.* **2013**, *139*.
- (22) Abrikosov, A. A.; Gorkov, P. L.; Dzyaloshinski, I. E. *Methods of quantum field theory in statistical physics*; Dover Publications INC. New York, 1975.
- (23) Mattuck, R. D. *A Guide to Feynman Diagrams in the Many-body Problem*, 2nd ed.; Dover Publications INC. New York, 1992.
- (24) Bruus, H.; Karsten, F. *Many-Body Quantum Theory in Condensed Matter Physics: An Introduction*; OUP Oxford: Oxford, 2004.
- (25) Martin, R. M.; Reining, L.; Ceperley, D. M. *Interacting electrons*; Cambridge University Press, 2016.

- (26) Klein, A. Perturbation theory for an infinite medium of fermions. *Phys. Rev.* **1961**, *121*, 950–956.
- (27) Luttinger, J. M.; Ward, J. C. Ground-state energy of a many-fermion system. II. *Phys. Rev.* **1960**, *118*, 1417–1427.
- (28) Kohn, W.; Sham, L. J., Self-Consistent Equations Including Exchange and Correlation Effects. *Phys. Rev.* **1965**, *140*, A1133.
- (29) Hohenberg, P.; Kohn, W. Inhomogeneous Electron Gas. *Phys. Rev.* **1964**, *136*, 864–871.
- (30) Casida, M. E. Generalization of the optimized-effective-potential model to include electron correlation: A variational derivation of the Sham-Schlüter equation for the exact exchange-correlation potential. *Phys. Rev. A* **1995**, *51*, 2005–2013.
- (31) Dahlen, N. E.; van Leeuwen, R.; von Barth, U. Variational energy functionals of the Green function and of the density tested on molecules. *Phys. Rev. A - At. Mol. Opt. Phys.* **2006**, *73*, 012511.
- (32) Hedin, L. New method for calculating the one-particle Green’s function with application to the electron-gas problem. *Phys. Rev.* **1965**, *139*, A796.
- (33) The pair bubble approximation is typically also denoted as RPA. To avoid potential confusion with the expression for the correlation energy, we will use the term bubble approximation when referring to the screening.
- (34) Sedlak, R.; Janowski, T.; Pitoňák, M.; Řezáč, J.; Pulay, P.; Hobza, P. Accuracy of quantum chemical methods for large noncovalent complexes. *J. Chem. Theory Comput.* **2013**, *9*, 3364–3374.
- (35) Řezáč, J.; Hobza, P. Benchmark Calculations of Interaction Energies in Noncovalent Complexes and Their Applications. *Chem. Rev.* **2016**, *116*, 5038–5071.

- (36) Dobson, J. F. Beyond pairwise additivity in London dispersion interactions. *Int. J. Quantum Chem.* **2014**, *114*, 1157–1161.
- (37) Zhang, I. Y.; Grüneis, A. Coupled cluster theory in materials science. *Front. Mater.* **2019**, *6*.
- (38) Keller, E.; Tsatsoulis, T.; Reuter, K.; Margraf, J. T. Regularized second-order correlation methods for extended systems. *J. Chem. Phys.* **2022**, *156*.
- (39) Eshuis, H.; Yarkony, J.; Furche, F. Fast computation of molecular random phase approximation correlation energies using resolution of the identity and imaginary frequency integration. *J. Chem. Phys.* **2010**, *132*, 234114.
- (40) Wilhelm, J.; Seewald, P.; Del Ben, M.; Hutter, J. Large-Scale Cubic-Scaling Random Phase Approximation Correlation Energy Calculations Using a Gaussian Basis. *J. Chem. Theory Comput.* **2016**, *12*, 5851–5859.
- (41) Wilhelm, J.; Golze, D.; Talirz, L.; Hutter, J.; Pignedoli, C. A. Toward GW Calculations on Thousands of Atoms. *J. Phys. Chem. Lett.* **2018**, *9*, 306–312.
- (42) Wilhelm, J.; Seewald, P.; Golze, D. Low-scaling GW with benchmark accuracy and application to phosphorene nanosheets. *J. Chem. Theory Comput.* **2021**, *17*, 1662–1677.
- (43) Förster, A.; Visscher, L. Low-Order Scaling G0W0 by Pair Atomic Density Fitting. *J. Chem. Theory Comput.* **2020**, *16*, 7381–7399.
- (44) Duchemin, I.; Blase, X. Separable resolution-of-the-identity with all-electron Gaussian bases: Application to cubic-scaling RPA. *J. Chem. Phys.* **2019**, *150*, 174120.
- (45) Duchemin, I.; Blase, X. Cubic-Scaling All-Electron GW Calculations with a Separable Density-Fitting Space-Time Approach. *J. Chem. Theory Comput.* **2021**, *17*, 2383–2393.

- (46) Schurkus, H. F.; Ochsenfeld, C. Communication: An effective linear-scaling atomic-orbital reformulation of the random-phase approximation using a contracted double-Laplace transformation. *J. Chem. Phys.* **2016**, *144*, 031101.
- (47) Luenser, A.; Schurkus, H. F.; Ochsenfeld, C. Vanishing-Overhead Linear-Scaling Random Phase Approximation by Cholesky Decomposition and an Attenuated Coulomb-Metric. *J. Chem. Theory Comput.* **2017**, *13*, 1647–1655.
- (48) Vlček, V.; Rabani, E.; Neuhauser, D.; Baer, R. Stochastic GW Calculations for Molecules. *J. Chem. Theory Comput.* **2017**, *13*, 4997–5003.
- (49) Graf, D.; Beuerle, M.; Schurkus, H. F.; Luenser, A.; Savasci, G.; Ochsenfeld, C. Accurate and Efficient Parallel Implementation of an Effective Linear-Scaling Direct Random Phase Approximation Method. *J. Chem. Theory Comput.* **2018**, *14*, 2505–2515.
- (50) Kresse, G.; Harl, J. Accurate bulk properties from approximate many-body techniques. *Phys. Rev. Lett.* **2009**, *103*, 4–7.
- (51) Lu, D.; Nguyen, H. V.; Galli, G. Power series expansion of the random phase approximation correlation energy: The role of the third- and higher-order contributions. *J. Chem. Phys.* **2010**, *133*.
- (52) Lebègue, S.; Harl, J.; Gould, T.; Ángyán, J. G.; Kresse, G.; Dobson, J. F. Cohesive properties and asymptotics of the dispersion interaction in graphite by the random phase approximation. *Phys. Rev. Lett.* **2010**, *105*, 1–4.
- (53) Eshuis, H.; Furche, F. A parameter-free density functional that works for noncovalent interactions. *J. Phys. Chem. Lett.* **2011**, *2*, 983–989.
- (54) Modrzejewski, M.; Yourdkhani, S.; Klimeš, J. Random Phase Approximation Applied to Many-Body Noncovalent Systems. *J. Chem. Theory Comput.* **2020**, *16*, 427–442.

- (55) Nguyen, B. D.; Chen, G. P.; Agee, M. M.; Burow, A. M.; Tang, M. P.; Furche, F. Divergence of Many-Body Perturbation Theory for Noncovalent Interactions of Large Molecules. *J. Chem. Theory Comput.* **2020**, *16*, 2258–2273.
- (56) Irmeler, A.; Gallo, A.; Hummel, F.; Grüneis, A. Duality of Ring and Ladder Diagrams and Its Importance for Many-Electron Perturbation Theories. *Phys. Rev. Lett.* **2019**, *123*, 156401.
- (57) Hummel, F.; Grüneis, A.; Kresse, G.; Ziesche, P. Screened Exchange Corrections to the Random Phase Approximation from Many-Body Perturbation Theory. *J. Chem. Theory Comput.* **2019**, *15*, 3223–3236.
- (58) Singwi, K. S.; Tosi, M. P.; Land, R. H.; Sjölander, A. Electron correlations at metallic densities. *Phys. Rev.* **1968**, *176*, 589–599.
- (59) Jiang, H.; Engel, E. Random-phase-approximation-based correlation energy functionals: Benchmark results for atoms. *J. Chem. Phys.* **2007**, *127*, 184108.
- (60) Lochan, R. C.; Head-Gordon, M. Orbital-optimized opposite-spin scaled second-order correlation: An economical method to improve the description of open-shell molecules. *J. Chem. Phys.* **2007**, *126*, 164101.
- (61) Neese, F.; Schwabe, T.; Kossmann, S.; Schirmer, B.; Grimme, S. Assessment of orbital-optimized, spin-component scaled second-order many-body perturbation theory for thermochemistry and kinetics. *J. Chem. Theory Comput.* **2009**, *5*, 3060–3073.
- (62) Kossmann, S.; Neese, F. Correlated ab initio spin densities for larger molecules: Orbital-optimized spin-component-scaled MP2 method. *J. Phys. Chem. A* **2010**, *114*, 11768–11781.
- (63) Grüneis, A.; Marsman, M.; Kresse, G. Second-order Møller-Plesset perturbation the-

- ory applied to extended systems. II. Structural and energetic properties. *J. Chem. Phys.* **2010**, *133*.
- (64) van Schilfgaarde, M.; Kotani, T.; Faleev, S. Quasiparticle self-consistent GW theory. *Phys. Rev. Lett.* **2006**, *96*, 226402.
- (65) Tal, A.; Chen, W.; Pasquarello, A. Vertex function compliant with the Ward identity for quasiparticle self-consistent calculations beyond GW. *Phys. Rev. B* **2021**, *103*, 161104.
- (66) Jung, Y.; Lochan, R. C.; Dutoi, A. D.; Head-Gordon, M. Scaled opposite-spin second order moller-pleeset correlation energy: An economical electronic structure method. *J. Chem. Phys.* **2004**, *121*, 9793–9802.
- (67) Lochan, R. C.; Jung, Y.; Head-Gordon, M. Scaled opposite spin second order Møller-Plesset theory with improved physical description of long-range dispersion interactions. *J. Phys. Chem. A* **2005**, *109*, 7598–7605.
- (68) Grimme, S. Improved second-order Møller-Plesset perturbation theory by separate scaling of parallel- and antiparallel-spin pair correlation energies. *J. Chem. Phys.* **2003**, *118*, 9095–9102.
- (69) Szabados, Á. Theoretical interpretation of Grimme’s spin-component-scaled second order Møller-Plesset theory. *J. Chem. Phys.* **2006**, *125*.
- (70) Pitoňák, M.; Neogrády, P.; Černý, J.; Grimme, S.; Hobza, P. Scaled MP3 non-covalent interaction energies agree closely with accurate CCSD(T) benchmark data. *ChemPhysChem* **2009**, *10*, 282–289.
- (71) Sedlak, R.; Riley, K. E.; Řezáč, J.; Pitoňák, M.; Hobza, P. MP2.5 and MP2.X: Approaching CCSD(T) quality description of noncovalent interaction at the cost of a single CCSD iteration. *ChemPhysChem* **2013**, *14*, 698–707.

- (72) Goldey, M.; Head-Gordon, M. Attenuating away the errors in inter- and intramolecular interactions from second-order Møller-plesset calculations in the small aug-cc-pVDZ basis set. *J. Phys. Chem. Lett.* **2012**, *3*, 3592–3598.
- (73) Goldey, M.; Dutoi, A.; Head-Gordon, M. Attenuated second-order Møller-Plesset perturbation theory: Performance within the aug-cc-pVTZ basis. *Phys. Chem. Chem. Phys.* **2013**, *15*, 15869–15875.
- (74) Goldey, M. B.; Belzunces, B.; Head-Gordon, M. Attenuated MP2 with a Long-Range Dispersion Correction for Treating Nonbonded Interactions. *J. Chem. Theory Comput.* **2015**, *11*, 4159–4168.
- (75) Lee, J.; Head-Gordon, M. Regularized Orbital-Optimized Second-Order Møller-Plesset Perturbation Theory: A Reliable Fifth-Order-Scaling Electron Correlation Model with Orbital Energy Dependent Regularizers. *J. Chem. Theory Comput.* **2018**, *14*, 5203–5219.
- (76) Pittner, J. Continuous transition between Brillouin-Wigner and Rayleigh-Schrödinger perturbation theory, generalized Bloch equation, and Hilbert space multireference coupled cluster. *J. Chem. Phys.* **2003**, *118*, 10876.
- (77) Engel, E.; Jiang, H. Orbital-Dependent Representation of the Correlation Energy Functional: Properties of Second-Order Kohn-Sham Perturbation Expansion. *Int. J. Quantum Chem.* **2006**, *106*, 3242–3259.
- (78) Jiang, H.; Engel, E. Kohn-Sham perturbation theory: Simple solution to variational instability of second order correlation energy functional. *J. Chem. Phys.* **2006**, *125*, 184108.
- (79) Daas, T. J.; Fabiano, E.; Della Sala, F.; Gori-Giorgi, P.; Vuckovic, S. Noncovalent Interactions from Models for the Møller-Plesset Adiabatic Connection. *J. Phys. Chem. Lett.* **2021**, *12*, 4867–4875.

- (80) Daas, T. J.; Kooi, D. P.; Grooteman, A. J. A. F.; Seidl, M.; Gori-Giorgi, P. Gradient Expansions for the Large-Coupling Strength Limit of the Møller–Plesset Adiabatic Connection. *J. Chem. Theory Comput.* **2022**, *18*, 1584–1594.
- (81) Kurth, S.; Perdew, J. P.; Blaha, P. Molecular and solid-state tests of density functional approximations: LSD, GGAs, and Meta-GGAs. *Int. J. Quantum Chem.* **1999**, *75*, 889–909.
- (82) Yan, Z.; Perdew, J. P.; Kurth, S. Density functional for short-range correlation: Accuracy of the random-phase approximation for isoelectronic energy changes. *Phys. Rev. B - Condens. Matter Mater. Phys.* **2000**, *61*, 16430–16439.
- (83) Angyan, J. G.; Gerber, I. C.; Savin, A.; Toulouse, J. Van der Waals forces in density functional theory: Perturbational long-range electron-interaction corrections. *Phys. Rev. A* **2005**, *72*, 012510.
- (84) Janesko, B. G.; Henderson, T. M.; Scuseria, G. E. Long-range-corrected hybrids including random phase approximation correlation. *J. Chem. Phys.* **2009**, *130*, 081105.
- (85) Janesko, B. G.; Henderson, T. M.; Scuseria, G. E. Long-range-corrected hybrid density functionals including random phase approximation correlation: Application to noncovalent interactions. *J. Chem. Phys.* **2009**, *131*, 034110.
- (86) Toulouse, J.; Gerber, I. C.; Jansen, G.; Savin, A.; Ángyán, J. G. Adiabatic-connection fluctuation-dissipation density-functional theory based on range separation. *Phys. Rev. Lett.* **2009**, *102*, 096404.
- (87) Zhu, W.; Toulouse, J.; Savin, A.; Ángyán, J. G. Range-separated density-functional theory with random phase approximation applied to noncovalent intermolecular interactions. *J. Chem. Phys.* **2010**, *132*, 244108.

- (88) Toulouse, J.; Zhu, W.; Ángyán, J. G.; Savin, A. Range-separated density-functional theory with the random-phase approximation: Detailed formalism and illustrative applications. *Phys. Rev. A - At. Mol. Opt. Phys.* **2010**, *82*, 032502.
- (89) Toulouse, J.; Zhu, W.; Savin, A.; Jansen, G.; Ángyán, J. G. Closed-shell ring coupled cluster doubles theory with range separation applied on weak intermolecular interactions. *J. Chem. Phys.* **2011**, *135*, 084119.
- (90) Beuerle, M.; Ochsenfeld, C. Short-range second order screened exchange correction to RPA correlation energies. *J. Chem. Phys.* **2017**, *147*.
- (91) Ren, X.; Tkatchenko, A.; Rinke, P.; Scheffler, M. Beyond the random-phase approximation for the electron correlation energy: The importance of single excitations. *Phys. Rev. Lett.* **2011**, *106*, 153003.
- (92) Ren, X.; Rinke, P.; Scuseria, G. E.; Scheffler, M. Renormalized second-order perturbation theory for the electron correlation energy: Concept, implementation, and benchmarks. *Phys. Rev. B - Condens. Matter Mater. Phys.* **2013**, *88*, 035120.
- (93) Hellgren, M.; Von Barth, U. Correlation potential in density functional theory at the GWA level: Spherical atoms. *Phys. Rev. B - Condens. Matter Mater. Phys.* **2007**, *76*, 1–12.
- (94) Hellgren, M.; Von Barth, U. Linear density response function within the time-dependent exact-exchange approximation. *Phys. Rev. B - Condens. Matter Mater. Phys.* **2008**, *78*, 1–10.
- (95) Heßelmann, A.; Görling, A. Random phase approximation correlation energies with exact Kohn-Sham exchange. *Mol. Phys.* **2010**, *108*, 359–372.
- (96) Heßelmann, A.; Görling, A. Correct description of the bond dissociation limit with-

- out breaking spin symmetry by a random-phase-approximation correlation functional. *Phys. Rev. Lett.* **2011**, *106*, 1–4.
- (97) Bates, J. E.; Furche, F. Communication: Random phase approximation renormalized many-body perturbation theory. *J. Chem. Phys.* **2013**, *139*, 171103.
- (98) Bleiziffer, P.; Krug, M.; Görling, A. Self-consistent Kohn-Sham method based on the adiabatic-connection fluctuation-dissipation theorem and the exact-exchange kernel. *J. Chem. Phys.* **2015**, *142*.
- (99) Mussard, B.; Rocca, D.; Jansen, G.; Ángyán, J. G. Dielectric Matrix Formulation of Correlation Energies in the Random Phase Approximation: Inclusion of Exchange Effects. *J. Chem. Theory Comput.* **2016**, *12*, 2191–2202.
- (100) Erhard, J.; Bleiziffer, P.; Görling, A. Power Series Approximation for the Correlation Kernel Leading to Kohn-Sham Methods Combining Accuracy, Computational Efficiency, and General Applicability. *Phys. Rev. Lett.* **2016**, *117*, 1–6.
- (101) Olsen, T.; Patrick, C. E.; Bates, J. E.; Ruzsinszky, A.; Thygesen, K. S. Beyond the RPA and GW methods with adiabatic xc-kernels for accurate ground state and quasi-particle energies. *Nat. Comput. Mater.* **2019**, *5*, 106.
- (102) Görling, A. Hierarchies of methods towards the exact Kohn-Sham correlation energy based on the adiabatic-connection fluctuation-dissipation theorem. *Phys. Rev. B* **2019**, *99*.
- (103) Maggio, E.; Kresse, G. Correlation energy for the homogeneous electron gas: Exact Bethe-Salpeter solution and an approximate evaluation. *Phys. Rev. B* **2016**, *93*, 1–12.
- (104) Holzer, C.; Gui, X.; Harding, M. E.; Kresse, G.; Helgaker, T.; Klopper, W. Bethe-Salpeter correlation energies of atoms and molecules. *J. Chem. Phys.* **2018**, *149*.

- (105) Loos, P.-F.; Scemama, A.; Duchemin, I.; Jacquemin, D.; Blase, X. Pros and Cons of the Bethe-Salpeter Formalism for Ground-State Energies. *J. Phys. Chem. Lett.* **2020**, *11*, 3536–3545.
- (106) Trushin, E.; Thierbach, A.; Görling, A. Toward chemical accuracy at low computational cost: Density-functional theory with σ -functionals for the correlation energy. *J. Chem. Phys.* **2021**, *154*.
- (107) Fauser, S.; Trushin, E.; Neiss, C.; Görling, A. Chemical accuracy with σ -functionals for the Kohn-Sham correlation energy optimized for different input orbitals and eigenvalues. *J. Chem. Phys.* **2021**, *155*.
- (108) Colonna, N.; Hellgren, M.; De Gironcoli, S. Correlation energy within exact-exchange adiabatic connection fluctuation-dissipation theory: Systematic development and simple approximations. *Phys. Rev. B - Condens. Matter Mater. Phys.* **2014**, *90*, 1–10.
- (109) Colonna, N.; Hellgren, M.; De Gironcoli, S. Molecular bonding with the RPAX: From weak dispersion forces to strong correlation. *Phys. Rev. B* **2016**, *93*, 1–11.
- (110) Hellgren, M.; Colonna, N.; De Gironcoli, S. Beyond the random phase approximation with a local exchange vertex. *Phys. Rev. B* **2018**, *98*, 1–12.
- (111) Hellgren, M.; Baguet, L. Random phase approximation with exchange for an accurate description of crystalline polymorphism. *Phys. Rev. Res.* **2021**, *3*.
- (112) Sharp, T.; Horton, G. A Variational Approach to the Unipotential Many-Electron Problem. *Phys. Rev.* **1953**, *90*, 317.
- (113) Talman, J. D.; Shadwick, W. F. Optimized effective atomic central potential. *Phys. Rev. A* **1976**, *14*, 36–40.
- (114) Engel, Eberhard and Dreizler, R. M. *Density functional theory An Advanced Course*; Springer, 2013.

- (115) Freeman, D. Coupled-cluster expansion applied to the electron gas: Inclusion of ring and exchange effects. *Phys. Rev. B* **1977**, *15*, 5512–5521.
- (116) Jansen, G.; Liu, R. F.; Ángyán, J. G. On the equivalence of ring-coupled cluster and adiabatic connection fluctuation-dissipation theorem random phase approximation correlation energy expressions. *J. Chem. Phys.* **2010**, *133*.
- (117) Paier, J.; Janesko, B. G.; Henderson, T. M.; Scuseria, G. E.; Grüneis, A.; Kresse, G. Hybrid functionals including random phase approximation correlation and second-order screened exchange. *J. Chem. Phys.* **2010**, *132*.
- (118) Grüneis, A.; Marsman, M.; Harl, J.; Schimka, L.; Kresse, G. Making the random phase approximation to electronic correlation accurate. *J. Chem. Phys.* **2009**, *131*, 154115.
- (119) Förster, A.; Visscher, L. Exploring the statically screened G3W2 correction to the GW self-energy : Charged excitations and total energies of finite systems. *Phys. Rev. B* **2022**, *105*, 125121.
- (120) Grüneis, A.; Kresse, G.; Hinuma, Y.; Oba, F. Ionization potentials of solids: The importance of vertex corrections. *Phys. Rev. Lett.* **2014**, *112*, 096401.
- (121) Řezáč, J.; Riley, K. E.; Hobza, P. S66: A well-balanced database of benchmark interaction energies relevant to biomolecular structures. *J. Chem. Theory Comput.* **2011**, *7*, 2427–2438.
- (122) Rieger, M. M.; Steinbeck, L.; White, I. D.; Rojas, H. N.; Godby, R. W. GW space-time method for the self-energy of large systems. *Comput. Phys. Commun.* **1999**, *117*, 211–228.
- (123) Dyson, F. J. The S matrix in quantum electrodynamics. *Phys. Rev.* **1949**, *75*, 1736–1755.

- (124) Baym, G.; Kadanoff, L. P. Conservation laws and correlation functions. *Phys. Rev.* **1961**, *124*, 287–299.
- (125) Salpeter, E. E.; Bethe, H. A. A relativistic equation for bound-state problems. *Phys. Rev.* **1951**, *84*, 1232–1242.
- (126) Starke, R.; Kresse, G. Self-consistent Green function equations and the hierarchy of approximations for the four-point propagator. *Phys. Rev. B* **2012**, *85*, 1–9.
- (127) Held, K.; Taranto, C.; Rohringer, G.; Toschi, A. In *LDA+DMFT approach to strongly Correl. Mater.*; Pavarini, E., Koch, E., Vollhardt, D., Lichtenstein, A., Eds.; 2011; Chapter 13, pp 13.1–13.22.
- (128) Hybertsen, M. S.; Louie, S. G. First-principles theory of quasiparticles: Calculation of band gaps in semiconductors and insulators. *Phys. Rev. Lett.* **1985**, *55*, 1418–1421.
- (129) Rohringer, G.; Valli, A.; Toschi, A. Local electronic correlation at the two-particle level. *Phys. Rev. B - Condens. Matter Mater. Phys.* **2012**, *86*.
- (130) Rohringer, G.; Hafermann, H.; Toschi, A.; Katanin, A. A.; Antipov, A. E.; Katsnelson, M. I.; Lichtenstein, A. I.; Rubtsov, A. N.; Held, K. Diagrammatic routes to nonlocal correlations beyond dynamical mean field theory. *Rev. Mod. Phys.* **2018**, *90*, 25003.
- (131) Romaniello, P.; Guyot, S.; Reining, L. The self-energy beyond GW: Local and nonlocal vertex corrections. *J. Chem. Phys.* **2009**, *131*, 154111.
- (132) Krien, F.; Kauch, A.; Held, K. Tiling with triangles: Parquet and GW γ methods unified. *Phys. Rev. Res.* **2021**, *3*, 13149.
- (133) van Leeuwen, R.; Dahlen, N. E.; Stefanucci, G.; Almladh, C. O.; Von Barth, U. In *Time-Dependent Density Funct. Theory*; Marques, M. A., Ullrich, C. A., Nogueira, F., Rubio, A., Burke, K., Gross, E. K., Eds.; Springer Heidelberg, 2015; pp 185–217.

- (134) Stefanucci, G.; Pavlyukh, Y.; Uimonen, A. M.; van Leeuwen, R. Diagrammatic expansion for positive spectral functions beyond GW: Application to vertex corrections in the electron gas. *Phys. Rev. B* **2014**, *90*, 115134.
- (135) Rodríguez-Mayorga, M.; Mitxelena, I.; Bruneval, F.; Piris, M. Coupling Natural Orbital Functional Theory and Many-Body Perturbation Theory by Using Nondynamically Correlated Canonical Orbitals. *J. Chem. Theory Comput.* **2021**, *17*, 7562–7574.
- (136) Baerends, E.; Ziegler, T.; Atkins, A.; Autschbach, J.; Baseggio, O.; Bashford, D.; Bérces, A.; Bickelhaupt, F.; Bo, C.; Boerrigter, P.; Cavallo, L.; Daul, C.; Chong, D.; Chulhai, D.; Deng, L.; Dickson, R.; Dieterich, J.; Ellis, D.; van Faassen, M.; Fan, L.; Fischer, T.; Förster, A.; Guerra, C. F.; Franchini, M.; Ghysels, A.; Giammona, A.; van Gisbergen, S.; Goetz, A.; Götz, A.; Groeneveld, J.; Gritsenko, O.; Grüning, M.; Gusarov, S.; Harris, F.; van den Hoek, P.; Hu, Z.; Jacob, C.; Jacobsen, H.; Jensen, L.; Joubert, L.; Kaminski, J.; van Kessel, G.; König, C.; Kootstra, F.; Kovalenko, A.; Krykunov, M.; van Lenthe, E.; McCormack, D.; Michalak, A.; Mitoraj, M.; Morton, S.; Neugebauer, J.; Nicu, V.; Noodleman, L.; Osinga, V.; Patchkovskii, S.; Pavanello, M.; Peeples, C.; Philipson, P.; Post, D.; Pye, C.; Ramanantoanina, H.; Ramos, P.; Ravenek, W.; Reimann, M.; Rodríguez, J.; Ros, P.; Rüger, R.; Schipper, P.; Schlüns, D.; van Schoot, H.; Schreckenbach, G.; Seldenthuis, J.; Seth, M.; Snijders, J.; Solà, M.; Stener, M.; Swart, M.; Swerhone, D.; Tognetti, V.; te Velde, G.; Vernooijs, P.; Versluis, L.; Visscher, L.; Visser, O.; Wang, F.; Wesolowski, T.; van Wezenbeek, E.; Wiesenekker, G.; Wolff, S.; Woo, T.; Yakovlev, A. ADF2022.1, locally modified development version. 2022.
- (137) Förster, A.; Visscher, L. GW100: A Slater-Type Orbital Perspective. *J. Chem. Theory Comput.* **2021**, *17*, 5080–5097.
- (138) Krykunov, M.; Ziegler, T.; Van Lenthe, E. Hybrid density functional calculations of

- nuclear magnetic shieldings using slater-type orbitals and the zeroth-order regular approximation. *Int. J. Quantum Chem.* **2009**, *109*, 1676–1683.
- (139) Wirz, L. N.; Reine, S. S.; Pedersen, T. B. On Resolution-of-the-Identity Electron Repulsion Integral Approximations and Variational Stability. *J. Chem. Theory Comput.* **2017**, *13*, 4897–4906.
- (140) Förster, A.; Franchini, M.; van Lenthe, E.; Visscher, L. A Quadratic Pair Atomic Resolution of the Identity Based SOS-AO-MP2 Algorithm Using Slater Type Orbitals. *J. Chem. Theory Comput.* **2020**, *16*, 875 – 891.
- (141) Kaltak, M.; Klimeš, J.; Kresse, G. Low scaling algorithms for the random phase approximation: Imaginary time and laplace transformations. *J. Chem. Theory Comput.* **2014**, *10*, 2498–2507.
- (142) Kaltak, M.; Klimeš, J.; Kresse, G. Cubic scaling algorithm for the random phase approximation: Self-interstitials and vacancies in Si. *Phys. Rev. B* **2014**, *90*, 054115.
- (143) Liu, P.; Kaltak, M.; Klimeš, J.; Kresse, G. Cubic scaling GW: Towards fast quasiparticle calculations. *Phys. Rev. B* **2016**, *94*, 165109.
- (144) Helgaker, T.; Klopper, W.; Koch, H.; Noga, J. Basis-set convergence of correlated calculations on water. *J. Chem. Phys.* **1997**, *106*, 9639–9646.
- (145) Jensen, F. Atomic orbital basis sets. *Wiley Interdiscip. Rev. Comput. Mol. Sci.* **2013**, *3*, 273–295.
- (146) Hellgren, M.; Rohr, D. R.; Gross, E. K. Correlation potentials for molecular bond dissociation within the self-consistent random phase approximation. *J. Chem. Phys.* **2012**, *136*.
- (147) Verma, P.; Bartlett, R. J. Increasing the applicability of density functional theory. II.

- Correlation potentials from the random phase approximation and beyond. *J. Chem. Phys.* **2012**, *136*.
- (148) Bleiziffer, P.; Heßelmann, A.; Görling, A. Efficient self-consistent treatment of electron correlation within the random phase approximation. *J. Chem. Phys.* **2013**, *139*.
- (149) Klimeš, J.; Kresse, G. Kohn-Sham band gaps and potentials of solids from the optimised effective potential method within the random phase approximation. *J. Chem. Phys.* **2014**, *140*, 054516.
- (150) Hellgren, M.; Caruso, F.; Rohr, D. R.; Ren, X.; Rubio, A.; Scheffler, M.; Rinke, P. Static correlation and electron localization in molecular dimers from the self-consistent RPA and GW approximation. *Phys. Rev. B - Condens. Matter Mater. Phys.* **2015**, *91*, 165110.
- (151) Voora, V. K.; Balasubramani, S. G.; Furche, F. Variational generalized Kohn-Sham approach combining the random-phase-approximation and Green's-function methods. *Phys. Rev. A* **2019**, *99*, 012518.
- (152) Graf, D.; Ochsenfeld, C. A range-separated generalized Kohn-Sham method including a long-range nonlocal random phase approximation correlation potential. *J. Chem. Phys.* **2020**, *153*.
- (153) Riemelmoser, S.; Kaltak, M.; Kresse, G. Optimized effective potentials from the random-phase approximation: Accuracy of the quasiparticle approximation. *J. Chem. Phys.* **2021**, *154*, 154103.
- (154) Yu, J. M.; Tsai, J.; Hernandez, D. J.; Furche, F.; Tsai, J.; Hernandez, D. J. Selfconsistent random phase approximation methods. *J. Chem. Phys.* **2021**, *155*, 040902.
- (155) Caruso, F.; Dauth, M.; Van Setten, M. J.; Rinke, P. Benchmark of GW Approaches for the GW100 Test Set. *J. Chem. Theory Comput.* **2016**, *12*, 5076–5087.

- (156) Kutepov, A. L. Electronic structure of Na, K, Si, and LiF from self-consistent solution of Hedin's equations including vertex corrections. *Phys. Rev. B* **2016**, *94*, 155101.
- (157) Santra, G.; Sylvetsky, N.; Martin, J. M. Minimally Empirical Double-Hybrid Functionals Trained against the GMTKN55 Database: RevDSD-PBEP86-D4, revDOD-PBE-D4, and DOD-SCAN-D4. *J. Phys. Chem. A* **2019**, *123*, 5129–5143.
- (158) Mehta, N.; Casanova-Páez, M.; Goerigk, L. Semi-empirical or non-empirical double-hybrid density functionals: Which are more robust? *Phys. Chem. Chem. Phys.* **2018**, *20*, 23175–23194.
- (159) Grimme, S.; Antony, J.; Ehrlich, S.; Krieg, H. A consistent and accurate ab initio parametrization of density functional dispersion correction (DFT-D) for the 94 elements H-Pu. *J. Chem. Phys.* **2010**, *132*, 154104.
- (160) Grimme, S.; Ehrlich, S.; Goerigk, L. Effect of the damping function in dispersion corrected density functional theory. *J. Comput. Chem.* **2011**, *32*, 1456–1465.
- (161) Ward, J. C. An Identity in Quantum Electrodynamics. *Phys. Rev.* **1950**, *78*, 182.
- (162) Kotani, T.; van Schilfhaarde, M.; Faleev, S. V. Quasiparticle self-consistent GW method: A basis for the independent-particle approximation. *Phys. Rev. B* **2007**, *76*, 165106.
- (163) Strinati, G. Application of the Green's functions method to the study of the optical properties of semiconductors. *La Riv. Del Nuovo Cim. Ser. 3* **1988**, *11*, 1–86.
- (164) Nakashima, T.; Raebiger, H.; Ohno, K. Normalization of exact quasiparticle wave functions in the Green's function method guaranteed by the Ward identity. *Phys. Rev. B* **2021**, *104*, L201116.
- (165) Bates, J. E.; Sengupta, N.; Sensenig, J.; Ruzsinszky, A. Adiabatic Connection without Coupling Constant Integration. *J. Chem. Theory Comput.* **2018**, *14*, 2979–2990.

- (166) Vlček, V. Stochastic Vertex Corrections: Linear Scaling Methods for Accurate Quasi-particle Energies. *J. Chem. Theory Comput.* **2019**, 6254–6266.
- (167) Doser, B.; Lambrecht, D. S.; Kussmann, J.; Ochsenfeld, C. Linear-scaling atomic orbital-based second-order Møller-Plesset perturbation theory by rigorous integral screening criteria. *J. Chem. Phys.* **2009**, 130, 064107.
- (168) Pinski, P.; Riplinger, C.; Valeev, E. F.; Neese, F. Sparse maps - A systematic infrastructure for reduced-scaling electronic structure methods. I. An efficient and simple linear scaling local MP2 method that uses an intermediate basis of pair natural orbitals. *J. Chem. Phys.* **2015**, 143, 034108.
- (169) Nagy, P. R.; Samu, G.; Kállay, M. An Integral-Direct Linear-Scaling Second-Order Møller-Plesset Approach. *J. Chem. Theory Comput.* **2016**, 12, 4897–4914.
- (170) Ljungberg, M. P.; Koval, P.; Ferrari, F.; Foerster, D.; Sánchez-Portal, D. Cubic-scaling iterative solution of the Bethe-Salpeter equation for finite systems. *Phys. Rev. B - Condens. Matter Mater. Phys.* **2015**, 92, 1–18.

Graphical TOC Entry

